

UNCLASSIFIED

Defense Technical Information Center  
Compilation Part Notice

ADP010719

TITLE: NAL SST Arrow Wing with Oscillating Flap

DISTRIBUTION: Approved for public release, distribution unlimited

This paper is part of the following report:

TITLE: Verification and Validation Data for  
Computational Unsteady Aerodynamics [Donnees de  
verification et de valadation pour  
l'aerodynamique instationnaire numerique]

To order the complete compilation report, use: ADA390566

The component part is provided here to allow users access to individually authored sections of proceedings, annals, symposia, ect. However, the component should be considered within the context of the overall compilation report and not as a stand-alone technical report.

The following component part numbers comprise the compilation report:

ADP010704 thru ADP010735

UNCLASSIFIED

## 12. NAL SST ARROW WING WITH OSCILLATING FLAP

M. Tamayama, K. Saitoh, H. Matsushita and J. Nakamichi

NAL, Tokyo

### INTRODUCTION

A wind tunnel model of a SST( Supersonic Transport ) arrow wing was tested in transonic regime. The purpose of this experiment is to accumulate verification data for the establishment of aeroelasticity related CFD codes and ACT ( Active Control Technology ) in the Japanese SST program.

The model is a semi-span arrow wing with a fuselage. The leading edge is double-swept-backed as shown in Fig. 1 and 2. The inboard sections of the model was constructed mainly with 7 mm thickness aluminum plate. A NACA0003 airfoil was, then, shaped by urethane resin. The dimensionless coordinates are shown in Table 1. At outboard sections, the NACA0003 airfoil was directly manufactured by cutting down an aluminum alloy. The detailed information on the model fuselage is shown in Table 2. Table 6 shows the model's natural frequencies acquired by both FEM analysis and a vibration test. Figure 5 shows the contours of model natural modes acquired by FEM analysis.

There is a flap, which can oscillate in the rear part of the inboard wing. The flap was driven by an electric motor around a hinge shaft which is parallel with the trailing edge. The deflection angle of the flap was measured using an appropriate transducer with installed inside the model fuselage. Downward motion was measured as positive angle.

Main measurement items presented here are pressures and deformations of the model. Steady and unsteady components of pressures were measured independently in order to remove the effect of thermal drift of pressure transducers. The pressure orifices are located at positions shown in Table 3 and Fig. 3. Chord positions in Table 3 are those for unsteady pressure transducers. The positions of steady pressure orifices are slightly different, because the span positions deviates 0.4% from the unsteady pressure orifices. The steady pressure orifice No.15 was not available because of the blockage of the vinyl tube, and it is not included in the experimental data provided.

The dynamic deformation of the model was measured by tracing optical targets installed in the wing surface. The positions of the optical targets are shown in Table 4 and Fig. 4. Multiple targets distributed in spanwise direction were measured with a single CCD camera. Four CCD cameras were used. While there were problems with the light intensity and some of the camera measurement systems failed, dynamic deformations were obtained at the target positions shown in Table 7.1. Four accelerometers are installed in the model. The locations are shown in Table 5 and Fig. 4. The accelerometer signals are useful for the verification of the dynamic deformation measurement system.

Tables 8.1 to 8.6 included in the accompanying CD-ROM show the results of steady and unsteady components of pressure coefficient, unsteady aerodynamic forces, steady and dynamic optical target displacement, and unsteady accelerometer signals. The unsteady results are presented only by the fundamental and 2nd harmonic components based on the flap frequency. The FFT function of Matlab was utilized in the frequency analysis. After data were FFT-processed in several intervals beginning from different time, they were averaged. The data length was double the sample frequency for each FFT-processing. The unsteady results presented in Tables 8.1 to 8.6 are not normalized by the flap amplitude. The phase characteristics are presented with respect to the flap motion. The results are also shown in Figs. 6, 7.1 to 7.12, 8.1, 8.2 and 9.1 to 9.6 (the whole set of figures is included in the accompanying CD-ROM here only some examples are presented). In these figures, only the fundamental component normalized by flap amplitude is shown.

### LIST OF SYMBOLS AND DEFINITIONS

|            |  |
|------------|--|
| $c$        | Local chord length   |
| $Cl$       | Unsteady section lift coefficient (normalized with $c$ )                           |
| $Cm$       | Unsteady section moment coefficient about 25% local chord (normalized with $c^2$ ) |
| $c_{mean}$ | Mean geometrical chord length (1.27 m)   |
| $Cp$       | Steady pressure coefficient  |
| $c_r$      | Root chord length  |

|                        |   |
|------------------------|---|
| $f$                    | Frequency   |
| $k$                    | Reduced frequency. $f\pi c_{mean}/U$                      |
| $M$                    | Free stream Mach number                                   |
| $P$                    | Unsteady Pressure above plenum chamber                    |
| $P'$                   | Real component of fundamental of $P$                      |
| $P''$                  | Imaginary component of fundamental of $P$                 |
| $P1'$                  | Real component of 2nd harmonic of $P$                     |
| $P1''$                 | Imaginary component of 2nd harmonic of $P$                |
| $P_o$                  | Free stream total pressure                                |
| $q$                    | Free stream dynamic pressure                              |
| $Re$                   | Reynolds number based on free stream conditions and $c_r$ |
| $s$                    | Semi-span width   |
| $T_o$                  | Free stream total temperature                             |
| $U$                    | Free stream velocity                                      |
| $x$                    | Chordwise coordinate                                      |
| $y$                    | Spanwise coordinate                                       |
| $z$                    | Model deformation   |
| $z'$                   | Real component of fundamental of $z$                      |
| $z''$                  | Imaginary component of fundamental of $z$                 |
| $z1'$                  | Real component of 2nd harmonic of $z$                     |
| $z1''$                 | Imaginary component of 2nd harmonic of $z$                |
| $\alpha$ ( alpha )     | Angle of incidence  |
| $\delta$ ( delta )     | Mean angle of flap deflection                             |
| $\delta_o$ ( delta_o ) | Amplitude of flap deflection                              |
| $\eta$ ( eta )         | Dimensionless spanwise coordinate, $y/s$                  |
| $\Lambda$ ( lambda )   | Sweepback angle   |
| $\xi$ ( xi )           | Dimensionless chordwise coordinate, $x/c$                 |
| $\theta$ ( theta )     | Phase lag of pressure with respect to flap motion         |

## FORMULARY

### 1 General Description of model

|                        |   |
|------------------------|---|
| 1.1 Designation        | NAL SST Arrow Wing with Fuselage                        |
| 1.2 Type               | Double swept-back semi-span model                       |
| 1.3 Derivation         | Proposed by Society of Japan Aircraft Company ( SJAC ). |
| 1.4 Additional remarks | ---   |
| 1.5 References         | Ref. 1, 2   |

### 2 Model Geometry

|  |  |
|--|--|
| 2.1 Planform   | Double tapered   |
| 2.2 Aspect ratio   | 2.01   |
| 2.3 Leading edge sweep   | 72.81 deg. ( inboard ) / 51.57 deg. ( outboard )   |
| 2.4 Trailing edge sweep  | 6.57 deg. ( inboard ) / 16.94 deg. ( outboard )  |
| 2.5 Taper ratio  | $1.0_{\eta=0\%} : 0.274_{57\%} : 0.0783_{100\%}$   |
| 2.6 Twist  | 0  |
| 2.7 Wing root chord  | 2103.3 mm  |
| 2.8 Semi-span of model   | 1000.0 mm ( From fuselage symmetry axis to wing tip. 35mm thickness base plate inserted between fuselage symmetry plane and tunnel side wall. See Table 2. )   |
| 2.9 Area of planform   | $0.8890 \text{ m}^2$ ( only wing ) [ fuselage : $0.2778 \text{ m}^2$ , base : $0.135 \text{ m}^2$ ]  |
| 2.10 Location of reference sections and definition of profiles | NACA0003 at 8 %, 57 % and 100 % semi-span positions ( see Table 1 )  |
| 2.11 Lofting procedure between reference sections              | Straight line generators   |
| 2.12 Form of wing-body junction                                | Wing root supported from 52.8 % to 81.4 % chord-stations at 3 points (see Fig. 2). Rest of root free to deform, so it presented vertical displacements when the wing oscillated. A 1 mm clearance was thus given between fuselage and wing root section without any fairing. |
| 2.13 Form of wing tip  | Fairing using complex curve at 100 % semi-span position ( semi-span length is slightly wider than 1000 mm. See Fig. 2 )  |
| 2.14 Control surface details                                   | Semi-span position : $\eta=20.0 - 50.0 \%$<br>Hinge-line : 110.0 mm upstream from trailing edge<br>Small chordwise and spanwise gaps (see Ref. 1 )   |
| 2.15 Additional remarks  | Wing surface consist of aluminum alloy and urethane resin. Accuracy of wing section shape considered within 0.25 and 1.0 mm respectively for aluminum and urethane surfaces.<br><br>Fuselage swell to cover the flap actuator presented in Table 2.                          |
| 2.16 References  | Ref. 1, 2  |

### 3 Wind Tunnel

|  |   |
|--|---|
| 3.1 Designation  | NAL 2m x 2m transonic wind tunnel   |
| 3.2 Type of tunnel   | Continuous and pressurized / depressurized  |
| 3.3 Test section dimensions                                    | Height : 2000 mm, Width : 2000 mm<br>Length : 4130 mm   |
| 3.4 Type of roof and floor                                     | Slotted   |
| 3.5 Type of side walls   | Closed  |
| 3.6 Ventilation geometry                                       | 6 slots on each of roof and floor. 6 % open ratio   |
| 3.7 Thickness of side wall boundary layer                      | ca. 0.1 m   |
| 3.8 Thickness of boundary layers at roof and floor             | ca. 0.1 m ( thicker than 0.1 m at slot sections )   |
| 3.9 Method of measuring Mach number                            | Derived from total and static pressures measured in settling and plenum chambers, respectively. Ratio of specific heats assumed 1.4.  |
| 3.10 Flow angularity   | Less than 0.1 deg. ( upwash ).  |
| 3.11 Uniformity of Mach number over test section               | Standard deviation of Mach number is less than 0.0025 for flow of Mach number less than 1.0.  |
| 3.12 Sources and levels of noise or turbulence in empty tunnel | At flow condition of $M=0.7$ , $P_o=98\text{kPa}$ and $T_o=310\text{K}$ , sound pressure levels based on $2 \times 10^{-5} \text{ Pa}$ are less than 130dB for each noise of 1st and 2nd fans and tunnel resonance. |
| 3.13 Tunnel resonances   | About 1 kHz corresponding to 1st natural frequency of test section plate.   |
| 3.14 Additional remarks  | ---   |
| 3.15 References on tunnel                                      | Ref. 3 and 4 written in Japanese  |

### 4 Model motion

|  |   |
|--|---|
| 4.1 General description  | Sinusoidal pitching of flap about swept hinge line  |
| 4.2 Definition of motion   | Flap deflection angle relative to hinge line measured with a cam attached to hinge axis and a depth meter installed in fuselage.  |
| 4.3 Range of amplitude   | Maximum command signal is 2 deg. with mean deflection angles of 0, 5 and -5 deg.  |
| 4.4 Range of frequency   | 0, 5, 10, 15( applied only to the mean deflection angle of 0 deg. ), 20, 25 and 30 Hz   |
| 4.5 Method of applying motion  | Forced by an electric motor   |
| 4.6 Timewise purity of motion  | Adequate purity of sinusoid   |
| 4.7 Natural frequencies and normal modes of model and support system | First bending frequency at 9.79 Hz and second bending frequency at 40.25 Hz with 3 point support. Analytic and tested results shown in Table 6. Analytic natural modes presented in Fig. 5.   |
| 4.8 Actual mode of applied motion including any elastic deformation  | Model dynamic deformation measured by observing optical targets installed in model. See Tables 8.1 to 8.6.<br><br>Model 1 <sup>st</sup> resonant frequency is almost 13.5 Hz with airflow. Flap oscillations at and below 15 Hz produce significant elastic deformations that influence unsteady pressure distributions and should be included in the calculations. Model deformation takes |

place most prominently in the 1<sup>st</sup> bending mode (Fig. 5). Detailed definition of the first 8 modes is included in the CD-ROM as file "FEM.txt"

|      |                    |           |
|------|--------------------|-----------|
| 4.9  | Additional remarks | ---       |
| 4.10 | References         | Ref. 1, 2 |

## 5 Test Conditions

|      |   |   |
|------|---|---|
| 5.1  | Model planform area/tunnel area                               | 0.222 (wing only). 0.325 (wing with fuselage and base plate)                          |
| 5.2  | Model span/tunnel width                                       | 0.500 ( wing and fuselage). 0.518 (model with base plate)                             |
| 5.3  | Blockage  | 1.27%   |
| 5.4  | Position of model in tunnel                                   | Side mounted at middle height   |
| 5.5  | Range of Mach number  | 0.80, 0.85, 0.90 and 0.95   |
| 5.6  | Range of tunnel total pressure                                | 70 and 80 kPa   |
| 5.7  | Range of tunnel total temperature                             | 306 to 315 deg. K   |
| 5.8  | Range of model steady or mean incidence                       | -4, -3, -2, -1, 0, 1 and 2 deg.   |
| 5.9  | Definition of model incidence                                 | Model set to zero incidence in horizontal plane.                                      |
| 5.10 | Position of transition, if free                               | Not measured  |
| 5.11 | Position and type of trip, if transition fixed                | ---   |
| 5.12 | Flow instabilities during tests                               | No remarkable instabilities detected.   |
| 5.13 | Changes to mean shape of model due to steady aerodynamic load | About 7.5 mm wing tip displacement at M=0.85 and Po=80 kPa.<br>See Tables 8.1 to 8.6. |
| 5.14 | Additional remarks  | ---   |
| 5.15 | References describing tests                                   | ---   |

## 6 Measurements and Observations

|      |   |                                      |
|------|---|--------------------------------------|
| 6.1  | Steady pressures for the mean conditions  | Available                            |
| 6.2  | Steady pressures for small changes from the mean conditions                     | Not Available                        |
| 6.3  | Quasi-steady pressures  | Not Available                        |
| 6.4  | Unsteady pressures  | Available                            |
| 6.5  | Steady section forces for the mean conditions by integration of pressures       | Not Available                        |
| 6.6  | Steady section forces for small changes from the mean conditions by integration | Not Available                        |
| 6.7  | Quasi-steady section forces by integration                                      | Not Available                        |
| 6.8  | Unsteady section forces by integration  | Available                            |
| 6.9  | Measurement of actual motion at points of model                                 | Available                            |
| 6.10 | Observation or measurement of boundary layer properties                         | Not Available                        |
| 6.11 | Visualisation of surface flow   | Not Available                        |
| 6.12 | Visualisation of shock wave movements   | Not Available                        |
| 6.13 | Additional remarks  | Accelerometer signals also measured. |

## 6.14 References

Ref. 2

**7 Instrumentation**

## 7.1 Steady pressure

## 7.1.1 Position of orifices

See Table 3 and Fig. 3

## 7.1.2 Type of measuring system

Orifices connected to scannivalves through vinyl tubes.

## 7.2 Unsteady pressure

## 7.2.1 Position of orifices

See Table 3 and Fig. 3

## 7.2.2 Diameter of orifices

1.0 mm

## 7.2.3 Type of measuring system

Individual in situ transducers

## 7.2.4 Type of transducers

Kulite XCS-062 range 15 PSI

## 7.2.5 Principle and accuracy of calibration

Steady calibration against DPI601 using reference tube of pressure transducer. Accuracy of the device is 0.05%.

## 7.3 Model motion

7.3.1 Method of measuring motion  
reference coordinates

Distance measured by depth meter mounted in fuselage and cam attached to hinge root.

7.3.2 Method of determining spatial mode  
of motion

Not measured for flap, but for wing itself. Optical targets set in the model were traced with CCD cameras. The position of targets presented in Table 4 and Fig. 4.

## 7.3.3 Accuracy of measured motion

Time response of angular transducer is less than 1 msec, which is equal to 10.8 deg. phase lag at 30 Hz flap motion. Accuracy of magnitude is less than 1 % taking into account non-linearity of depth meter and cam, and temperature characteristics of depth meter and its amplifier.

## 7.4 Processing of unsteady measurements

7.4.1 Method of acquiring and processing  
measurements

Pressure above the plenum chamber, accelerometer signal, flap control signal and its actual motion sampled simultaneously at 25.6 kHz and stored. Data processed off-line to 256 Hz. Dynamic model deformation measured by another system at 333 Hz and stored.

## 7.4.2 Type of analysis

Complex components of  $C_p$  using about 5 seconds data for each flap frequency. Averaging conducted. See INTRODUCTION.7.4.3 Unsteady pressure quantities obtained  
and accuracies achieved

Fundamental and 2nd harmonic components for each flap frequency presented. Although no unsteady calibrations were conducted, accuracy shown in 9.1.6 is expected.

## 7.4.4 Method of integration to obtain forces

Simpson method. Discretely divided distributions using spline interpolation. Leading edge unsteady  $C_p$  assumed to zero. At outboard section, trailing edge unsteady  $C_p$  assumed to mean of values extrapolated on each of upper and lower surfaces.

## 7.5 Additional remarks

4 accelerometers installed in wing ( see Table 5 and Fig. 4).

## 7.6 References on techniques

Ref. 1

**8 Data presentation**8.1 Test cases for which data could be made  
available

Table 7.2 (Included in accompanying CD-ROM)

|      |   |  |
|------|---|--|
| 8.2  | Test cases for which data are included in this document | Table 7.1  |
| 8.3  | Steady pressures  | Tables 8.1 to 8.6 (Included in accompanying CD-ROM)  |
| 8.4  | Quasi-steady or steady perturbation pressures           | ---  |
| 8.5  | Unsteady pressures                                      | Tables 8.1 to 8.6 (Included in accompanying CD-ROM)  |
| 8.6  | Steady forces or moments                                | ---  |
| 8.7  | Quasi-steady or unsteady perturbation forces            | ---  |
| 8.8  | Unsteady forces and moments                             | Tables 8.1 to 8.6 (Included in accompanying CD-ROM)  |
| 8.9  | Other forms in which data could be made available       | Static and dynamic model deformations presented in Tables 8.1 to 8.6. Accelerometer signals also presented in Tables 8.1 to 8.6. |
| 8.10 | Reference giving other representations of data          | ---  |

## 9 Comments on data

|       |   |  |
|-------|---|--|
| 9.1   | Accuracy  |  |
| 9.1.1 | Mach number   | Less than 0.001  |
| 9.1.2 | Steady incidence  | 0.1 deg.   |
| 9.1.3 | Reduced frequency   | Less than 0.12%  |
| 9.1.4 | Steady pressure coefficients  | Less than $(7.9 \times C_p^2 + 5.9)^{0.5} \times 0.001$  |
| 9.1.5 | Steady pressure derivatives   | ---  |
| 9.1.6 | Unsteady pressure coefficients  | Accuracy of $ P/q $ less than $(0.22 \times  P/q ^2 + 1.2)^{0.5} \times 0.01$ . Effects of repeatability and temperature sensitivity of pressure transducer and calibration error were considered.     |
| 9.2   | Sensitivity to small changes of parameter                             | Not examined   |
| 9.3   | Non-linearities   | Expansion waves seemed to appear only on the flap at higher Mach number.<br><br>Unsteady pressure distribution affected by non-linearity of dynamic model deformation at model 1st resonant frequency. |
| 9.4   | Influence of tunnel total pressure                                    | Total pressure of 70 and 80 kPa examined.  |
| 9.5   | Effects on data of uncertainty, or variation, in mode of model motion | Not estimated yet  |
| 9.6   | Wall interference corrections   | None   |
| 9.7   | Other relevant tests on same model                                    | Ref. 1   |
| 9.8   | Relevant tests on other models of nominally the same shapes           | ---  |
| 9.9   | Any remarks relevant to comparison between experiment and theory      | ---  |
| 9.10  | Additional remarks  | ---  |
| 9.11  | References on discussion of data                                      | Ref. 2   |

## 10 Personal contact for further information

Masato Tamayama

Aeroelasticity Laboratory, Structures Division

National Aerospace Laboratory



7-44-1, Jindaiji-Higashi-Machi,  
 Chofu, Tokyo 182-8522, JAPAN  
 Phone : +81-422-40-3392  
 Fax : +81-422-40-3376  
 E-mail : masato@nal.go.jp

## 11 List of references

- 1 M. Tamayama, H. Miwa, J. Nakamichi; Unsteady Aerodynamics Measurements on an Elastic Wing Model of SST, AIAA 97-0836, 1997
- 2 M. Tamayama, K. Saitoh, H. Matsushita; Measurements of Unsteady Pressure Distributions and Dynamic Deformations on an SST Elastic Wing Model, CEAS International Forum on Aeroelasticity and Structural Dynamics, Rome, Italy, 1997, Vol.3, pp.231-238.
- 3 N. Kawai, Y. Oguni, M. Suzuki; Measurements of Free-Stream Turbulence and Disturbance in NAL 2m x 2m Transonic Windtunnel, NAL TM-342, 1978 (in Japanese).
- 4 K. Suzuki, et al; Refurbishment of the NAL 2m x 2m Transonic Wind Tunnel Test Section, NAL TM-674, 1995 (in Japanese).

Table 1 Airfoil Section Shape

Airfoil NACA0003

$$z_t(\xi) / c = 5 \times 0.03 \times \{ a_0 \xi^{1/4} + a_1 \xi + a_2 \xi^2 + a_3 \xi^3 + a_4 \xi^4 \}$$

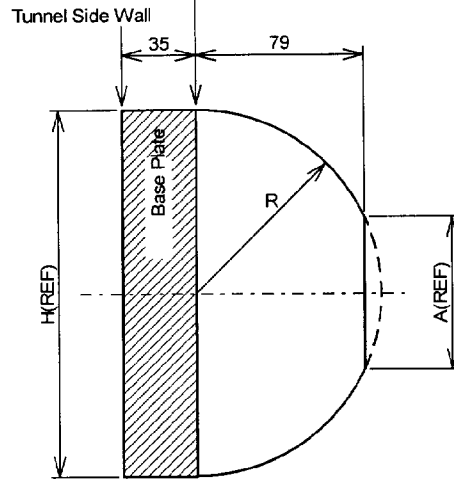
$$a_0 = 0.2969, a_1 = -0.1260, a_2 = -0.3516$$

$$a_3 = 0.2843, a_4 = -0.1015$$

$z_t(\xi)$ : Local airfoil thickness

| $\xi$ | $z_t(\xi)$ | $\xi$ | $z_t(\xi)$ |
|-------|------------|-------|------------|
| 0.00  | 0.00000    | 0.52  | 0.01291    |
| 0.04  | 0.00807    | 0.56  | 0.01220    |
| 0.08  | 0.01077    | 0.60  | 0.01141    |
| 0.12  | 0.01247    | 0.64  | 0.01055    |
| 0.16  | 0.01360    | 0.68  | 0.00964    |
| 0.20  | 0.01434    | 0.72  | 0.00867    |
| 0.24  | 0.01478    | 0.76  | 0.00764    |
| 0.28  | 0.01498    | 0.80  | 0.00656    |
| 0.32  | 0.01498    | 0.84  | 0.00542    |
| 0.36  | 0.01482    | 0.88  | 0.00423    |
| 0.40  | 0.01451    | 0.92  | 0.00299    |
| 0.44  | 0.01408    | 0.96  | 0.00168    |
| 0.48  | 0.01354    | 1.00  | 0.00031    |

Table 2 Definition of Fuselage  
0% Semi-Span

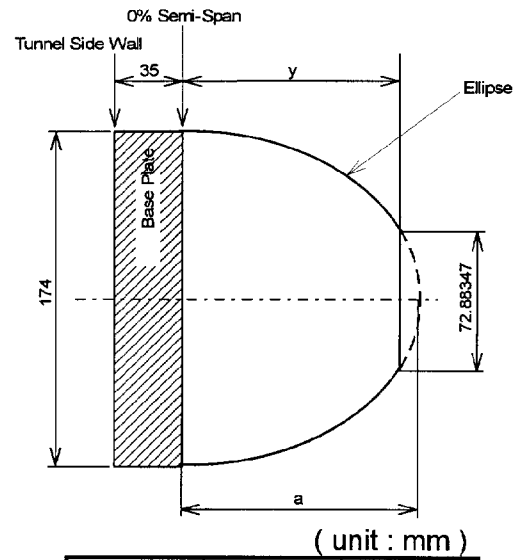


( unit : mm )

| STA                   | R                                   | H(REF) | A(REF) |
|-----------------------|-------------------------------------|--------|--------|
| -760                  | 0.00                                | 0.00   | -----  |
| -700                  | 15.31                               | 30.63  | -----  |
| -600                  | 36.65                               | 73.31  | -----  |
| -500                  | 53.27                               | 106.54 | -----  |
| -400                  | 65.76                               | 131.52 | -----  |
| -300                  | 74.71                               | 149.42 | -----  |
| -200                  | 80.71                               | 161.41 | 33.02  |
| -100                  | 84.34                               | 168.69 | 59.10  |
| 0                     | 86.21                               | 172.43 | 69.04  |
| 100                   | 86.90                               | 173.80 | 72.41  |
| 190                   | 87.00                               | 174.00 | 72.88  |
| 200<br>:<br>1700      | 87.00                               | 174.00 | 72.88  |
| 1824.4<br>:<br>2204.4 | *( control surface actuator swell ) |        |        |
| 2300<br>:<br>2400     | 87.00                               | 174.00 | 72.88  |
| 2500                  | 86.62                               | 173.24 | 71.05  |
| 2600                  | 84.04                               | 168.08 | 57.32  |
| 2700                  | 78.02                               | 156.04 | -----  |
| 2800                  | 68.56                               | 137.12 | -----  |
| 2900                  | 55.52                               | 111.04 | -----  |
| 3000                  | 37.32                               | 74.64  | -----  |
| 3100                  | 0.00                                | 0.00   | -----  |

The origin of STA is the wing leading edge  
at 8% semi-span position (wing-fuselage junction).

\*( control surface actuator swell )



| STA    | y      | a      |
|--------|--------|--------|
| 1824.4 | 80.00  | 88.10  |
| 1864.4 | 85.50  | 94.16  |
| 1904.4 | 95.50  | 105.17 |
| 1944.4 | 109.50 | 120.59 |
| 1984.4 | 115.00 | 126.64 |
| 2024.4 | 114.00 | 125.54 |
| 2064.4 | 107.00 | 117.83 |
| 2104.4 | 94.00  | 103.52 |
| 2144.4 | 84.00  | 92.51  |
| 2184.4 | 80.00  | 88.10  |
| 2204.4 | 79.50  | 87.55  |

Table 3 Pressure Orifice Locations

| $\eta = 38.4\%$ span ( Steady )<br>38% span ( Unsteady ) |         |               |         | $\eta = 73.5\%$ span ( Steady )<br>73.9% span ( Unsteady ) |         |               |         |
|--|---------|---------------|---------|--|---------|---------------|---------|
| Upper Surface  |         | Lower Surface |         | Upper Surface  |         | Lower Surface |         |
| ch   | x/c [%] | ch            | x/c [%] | ch   | x/c [%] | ch            | x/c [%] |
| 1  | 2.5     | 22            | 70.0    | 30   | 10.0    | 39            | 79.0    |
| 2  | 5.0     | 23            | 60.0    | 31   | 20.0    | 40            | 66.0    |
| 3  | 7.5     | 24            | 50.0    | 32   | 30.0    | 41            | 54.2    |
| 4  | 10.0    | 25            | 40.0    | 33   | 35.0    | 42            | 48.0    |
| 5  | 15.0    | 26            | 30.0    | 34   | 41.8    | 43            | 41.8    |
| 6  | 20.0    | 27            | 20.0    | 35   | 48.0    | 44            | 30.0    |
| 7  | 30.0    | 28            | 10.0    | 36   | 54.2    | 45            | 20.0    |
| 8  | 40.0    | 29            | 5.0     | 37   | 66.0    | 46            | 10.0    |
| 9  | 50.0    |               |         | 38   | 80.0    |               |         |
| 10   | 60.0    |               |         |  |         |               |         |
| 11   | 70.0    |               |         |  |         |               |         |
| 12   | 80.0    |               |         |  |         |               |         |
| 13   | 82.5    |               |         |  |         |               |         |
| 14   | 85.0    |               |         |  |         |               |         |
| 15   | 86.5*   |               |         |  |         |               |         |
| 16   | 88.0    |               |         |  |         |               |         |
| 17   | 91.6    |               |         |  |         |               |         |
| 18   | 93.1    |               |         |  |         |               |         |
| 19   | 94.6    |               |         |  |         |               |         |
| 20   | 96.1    |               |         |  |         |               |         |
| 21   | 100.0*  |               |         |  |         |               |         |

\* : Only for Unsteady Measurement

Table 4 Optical Target Locations

| No. | $\eta$<br>% | $\xi$<br>% | No.  | $\eta$<br>% | $\xi$<br>% |
|-----|-------------|------------|------|-------------|------------|
| * 1 | 96.0        | 13.0       | 11   | 41.0        | 43.2       |
| * 2 | 96.0        | 38.6       | 12   | 41.0        | 63.2       |
| 3   | 96.0        | 64.2       | * 13 | 41.0        | 74.0       |
| 4   | 76.0        | 28.2       | * 14 | 41.0        | 83.4       |
| * 5 | 76.0        | 48.5       | 15   | 18.0        | 38.2       |
| * 6 | 76.0        | 66.3       | 16   | 18.0        | 59.9       |
| 7   | 60.0        | 3.4        | * 17 | 18.0        | 73.0       |
| 8   | 60.0        | 41.4       | * 18 | 18.0        | 80.2       |
| * 9 | 60.0        | 59.1       | * 19 | 18.0        | 87.1       |
| 10  | 41.0        | 5.0        | * 20 | 60.0        | 74.5       |
|     |             |            | 21   | 18.0        | 20.6       |

\* Available

Table 5 Position of Accelerometers

| 66.8% Semi-Span |       | 84.7% Semi-Span |       |
|-----------------|-------|-----------------|-------|
| No.             | % x/c | No.             | % x/c |
| 1               | 30.0  | 2               | 30.0  |
| 3               | 65.0  | 4               | 65.0  |

Table 6 Model Natural Frequencies

| Mode | Natural Frequency[Hz] |                | Generalized Mass [ kg ] |
|------|-----------------------|----------------|-------------------------|
|      | FEM                   | Vibration Test |                         |
| 1    | 11.09                 | 9.79           | 5.1982                  |
| 2    | 41.65                 | ---            | 2.3109                  |
| 3    | 44.00                 | 40.25          | 3.2874                  |
| 4    | 56.26                 | 47.91          | 1.9764                  |
| 5    | 89.49                 | 65.19          | 1.4333                  |
| 6    | 119.23                | 90.57          | 0.7928                  |
| 7    | 145.44                | 111.04         | 2.0683                  |
| 8    | 163.58                | 122.39         | 1.2810                  |

Table 7.1 SUMMARY OF PRESENTED DATA

| Test ID No. | M      | Po [ kPa ] | To [°K] | Re x 10 <sup>-7</sup> | kf [ /Hz ] | f [ Hz ]              | α [°] | δ [°] | Target data available                 |
|-------------|--------|------------|---------|-----------------------|------------|-----------------------|-------|-------|---------------------------------------|
| AC100803    | 0.8002 | 79.925     | 310.36  | 2.142                 | 0.0150     | 5, 10, 15, 20, 25, 30 | 0     | 0     | 1, 2, 5, 6, 9, 13, 14, 18, 19, 20     |
| AC100804    | 0.8004 | 79.963     | 310.52  | 2.141                 | 0.0150     | 5, 10, 20, 25, 30     | 0     | 5     | 1, 2, 5, 6, 9, 20                     |
| AC100901    | 0.8507 | 80.000     | 310.34  | 2.207                 | 0.0143     | 5, 10, 15, 20, 25, 30 | 0     | 0     | 1, 2, 5, 6, 9, 13, 14, 17, 18, 19, 20 |
| AC100902    | 0.8489 | 79.936     | 310.78  | 2.199                 | 0.0143     | 5, 10, 20, 25, 30     | 0     | -5    | 1, 2, 5, 6, 9, 13, 14, 17, 18, 19, 20 |
| AC100907    | 0.9001 | 80.083     | 311.87  | 2.247                 | 0.0135     | 5, 10, 15, 20, 25, 30 | 0     | 0     | 1, 2, 5, 6, 9, 13, 14, 17, 18, 19, 20 |
| AC100908    | 0.9005 | 79.956     | 312.34  | 2.239                 | 0.0135     | 5, 10, 20, 25, 30     | 0     | 5     | 1, 2, 5, 6, 9, 13, 17, 18, 20         |

|   |
|---|
| Test No. AC100803                               |
| M = 0.8002, Po = 79.925 kPa, To = 310.36 deg. K |
| Re = 2.142*10 <sup>7</sup> , k/f = 0.0150 /Hz   |
| Alpha = 0 deg., Delta = 0 deg.                  |

[ STEADY DATA ]

< PRESSURE COEFFICIENT (Cp) >

$\eta = 38.4\%$

| Upper surface<br>Orifice No. | Lower surface |         |             | Upper surface |         |             | Lower surface |         |             |
|------------------------------|---------------|---------|-------------|---------------|---------|-------------|---------------|---------|-------------|
|                              | Xi            | Cp      | Orifice No. | Xi            | Cp      | Orifice No. | Xi            | Cp      | Orifice No. |
| 1                            | 0.025         | -0.0229 | 22          | 0.700         | -0.0458 | 30          | 0.100         | -0.1239 | 39          |
| 2                            | 0.050         | -0.0400 | 23          | 0.600         | -0.0551 | 31          | 0.200         | -0.1254 | 40          |
| 3                            | 0.075         | -0.0420 | 24          | 0.500         | -0.0605 | 32          | 0.300         | -0.0941 | 41          |
| 4                            | 0.100         | -0.0440 | 25          | 0.400         | -0.0545 | 33          | 0.350         | -0.0848 | 42          |
| 5                            | 0.150         | -0.0496 | 26          | 0.300         | -0.0600 | 34          | 0.418         | -0.0785 | 43          |
| 6                            | 0.200         | -0.0571 | 27          | 0.200         | -0.0529 | 35          | 0.480         | -0.0695 | 44          |
| 7                            | 0.300         | -0.0613 | 28          | 0.100         | -0.0403 | 36          | 0.542         | -0.0702 | 45          |
| 8                            | 0.400         | -0.0667 | 29          | 0.050         | -0.0563 | 37          | 0.660         | -0.0492 | 46          |
| 9                            | 0.500         | -0.0573 |             |               |         | 38          | 0.800         | -0.0448 |             |

&lt; DEFORMATION FROM NO-FLOW CONDITION &gt;

| Target No. |              |
|------------|--------------|
| 1          | +8.9354e-003 |
| 2          | +9.2979e-003 |
| 5          | +6.6282e-003 |
| 6          | +6.9474e-003 |
| 9          | +4.5407e-003 |
| 13         | +2.4733e-003 |
| 18         | +9.0811e-004 |
| 19         | +1.2350e-003 |
| 20         | +4.9521e-003 |
|            | { unit : m } |

[ UNSTEADY DATA ]

f = 5.0 Hz Delta\_o = 1.407 deg.  
< PRESSURE >

| No. | P'/q         | P'''/q       | P1'/q        | P1'''/q      | No. | P'/q         | P'''/q       | P1'/q        | P1'''/q      |
|-----|--------------|--------------|--------------|--------------|-----|--------------|--------------|--------------|--------------|
| 1   | +7.8672e-004 | +4.3709e-005 | +8.0516e-005 | -5.8224e-005 | 24  | -1.1412e-003 | +4.8577e-005 | -3.5234e-004 | -5.9388e-005 |
| 2   | +7.5615e-004 | +3.6843e-005 | +8.3222e-005 | -5.1448e-005 | 25  | -1.1946e-003 | +9.3217e-005 | -3.3515e-004 | -4.4607e-005 |
| 3   | +7.2296e-004 | +1.7149e-005 | +9.1091e-005 | -2.5512e-005 | 26  | -9.6874e-004 | +5.0285e-005 | -2.5858e-004 | -3.5429e-005 |
| 4   | +7.1944e-004 | +5.0864e-005 | +8.6095e-005 | -5.9453e-005 | 27  | -7.9342e-004 | +5.6215e-005 | -2.2098e-004 | -3.3815e-005 |
| 5   | +8.0283e-004 | +3.0358e-005 | +1.2223e-004 | -8.6025e-005 | 28  | -8.8828e-004 | +6.7967e-005 | -1.9143e-004 | -2.8182e-005 |
| 6   | +6.6100e-004 | +7.0002e-005 | +1.2902e-004 | -8.9684e-005 | 29  | -7.8033e-004 | +4.7247e-005 | -1.6621e-004 | -3.8227e-005 |
| 7   | +1.0015e-003 | +1.0361e-004 | +1.3800e-004 | -8.1173e-005 | 30  | +4.6798e-003 | +2.3276e-004 | +9.8975e-004 | -9.0601e-005 |
| 8   | +1.3027e-003 | +6.1052e-005 | +2.1992e-004 | -1.1785e-004 | 31  | +1.9328e-003 | +1.4899e-004 | +5.4238e-004 | -6.5775e-005 |
| 9   | +1.1805e-003 | +8.9660e-005 | +2.1234e-004 | -1.0954e-004 | 32  | +9.2340e-005 | +1.4845e-004 | +2.0084e-004 | -7.4948e-005 |
| 10  | +7.8312e-004 | +3.6655e-005 | +1.5814e-004 | -1.1425e-004 | 33  | -3.8883e-004 | +1.4808e-004 | +1.9665e-004 | -1.0070e-004 |
| 11  | +9.8334e-004 | -1.0328e-004 | -7.1924e-005 | -2.0106e-004 | 34  | -9.4809e-004 | +1.0313e-004 | +9.0647e-005 | -1.1219e-004 |
| 12  | -5.7040e-003 | -6.1674e-004 | -7.0427e-004 | -4.4130e-004 | 35  | -1.5268e-003 | +1.0638e-004 | -3.5361e-006 | -9.9731e-005 |
| 13  | -8.5204e-003 | -6.2376e-004 | -1.0955e-003 | -4.4207e-004 | 36  | -1.9714e-003 | +9.2792e-005 | -6.7405e-005 | -1.1752e-004 |
| 14  | -1.2701e-002 | -1.0577e-003 | -1.6996e-003 | -5.5173e-004 | 37  | -1.9822e-003 | +7.4661e-005 | -4.9516e-005 | -1.4588e-004 |
| 15  | -1.6012e-002 | -1.3849e-003 | -2.1815e-003 | -6.0164e-004 | 38  | -1.5498e-003 | +8.7056e-005 | -9.5056e-005 | -1.3375e-004 |
| 16  | -2.7111e-002 | -2.5209e-003 | -3.8842e-003 | -8.6146e-004 | 39  | +1.5977e-003 | +2.0498e-004 | -6.9301e-005 | -1.3918e-004 |
| 17  | -6.5368e-002 | -4.4412e-003 | -5.8103e-003 | -1.5791e-003 | 40  | +2.0575e-003 | +2.2058e-004 | -6.3125e-005 | -1.3469e-004 |
| 18  | -4.1524e-002 | -3.3402e-003 | -4.1162e-003 | -1.1320e-003 | 41  | +1.9475e-003 | +1.8157e-004 | -1.2719e-004 | -1.4087e-004 |
| 19  | -2.7545e-002 | -2.5878e-003 | -2.8568e-003 | -9.0288e-004 | 42  | +1.5229e-003 | +1.6212e-004 | -3.1213e-004 | -1.4390e-004 |
| 20  | -1.7642e-002 | -1.9067e-003 | -1.9389e-003 | -7.1725e-004 | 43  | +1.0206e-003 | +1.0437e-004 | -3.2457e-004 | -1.5941e-004 |
| 21  | +1.5456e-004 | +2.1606e-004 | +2.1787e-004 | -6.7360e-005 | 44  | -4.6880e-004 | +7.7942e-005 | -5.3641e-004 | -1.5246e-004 |
| 22  | +7.3478e-004 | +2.3072e-004 | -1.9087e-004 | -1.9774e-006 | 45  | -2.0729e-003 | +3.9180e-005 | -7.7220e-004 | -1.8623e-004 |
| 23  | -9.1626e-004 | +9.5325e-005 | -3.8716e-004 | -6.6705e-005 | 46  | -4.9538e-003 | -4.0297e-005 | -1.3125e-003 | -2.3554e-004 |

&lt; AERODYNAMIC FORCE &gt;

|             | real(fundamental) | imag(fundamental) | real(2nd harmonic) | imag(2nd harmonic) |
|-------------|-------------------|-------------------|--------------------|--------------------|
| C1 inboard  | +4.4811e-003      | +5.4617e-004      | +3.0432e-004       | +2.4205e-004       |
| C1 outboard | +1.9189e-004      | -2.9888e-006      | -5.3971e-004       | -4.7549e-005       |
| Cm inboard  | -3.5334e-003      | -3.4665e-004      | -3.4419e-004       | -1.3376e-004       |
| Cm outboard | -9.4222e-004      | -2.7897e-005      | -4.0941e-005       | +3.2761e-007       |

&lt; DYNAMIC DEFORMATION &gt;

| Target NO. | real(fundamental) | imag(fundamental) | real(2nd harmonic) | imag(2nd harmonic) |
|------------|-------------------|-------------------|--------------------|--------------------|
| 1          | +3.0206e-003      | -5.5430e-005      | +2.9867e-004       | -5.6899e-004       |
| 2          | +3.1819e-003      | -5.8974e-005      | +3.1358e-004       | -5.9964e-004       |
| 5          | +2.3323e-003      | -2.5983e-004      | +1.4506e-004       | -4.6065e-004       |
| 6          | +2.5142e-003      | -4.4531e-005      | +2.4202e-004       | -4.5089e-004       |
| 9          | +1.7175e-003      | -1.9038e-004      | +1.0799e-004       | -3.2052e-004       |
| 13         | +9.6971e-004      | -1.0812e-004      | +5.9302e-005       | -1.7505e-004       |
| 14         | +1.1849e-003      | -1.3701e-004      | +6.6696e-005       | -2.1126e-004       |
| 18         | +2.1879e-004      | -2.4470e-005      | +1.4574e-005       | -3.7917e-005       |
| 19         | +3.6009e-004      | -5.5330e-005      | +1.9597e-005       | -5.7822e-005       |
| 20         | +1.9133e-003      | -2.1409e-004      | +1.1434e-004       | -3.5716e-004       |

```

[ unit : m ]

< ACCELERATION >
Acc. NO.    real(fundamental)  imag(fundamental)  real(2nd harmonic)  imag(2nd harmonic)
1          -1.6517e+000        -1.0160e-001       -1.3742e+000        -1.0738e-001
2          -2.6439e+000        -1.7970e-001       -2.2206e+000        -1.5267e-001
3          -1.8257e+000        -4.7501e-002       -1.6589e+000        -1.1162e-001
4          -2.8493e+000        -1.5522e-001       -2.4137e+000        -1.4551e-001
[ unit : m/s^2 ]

```



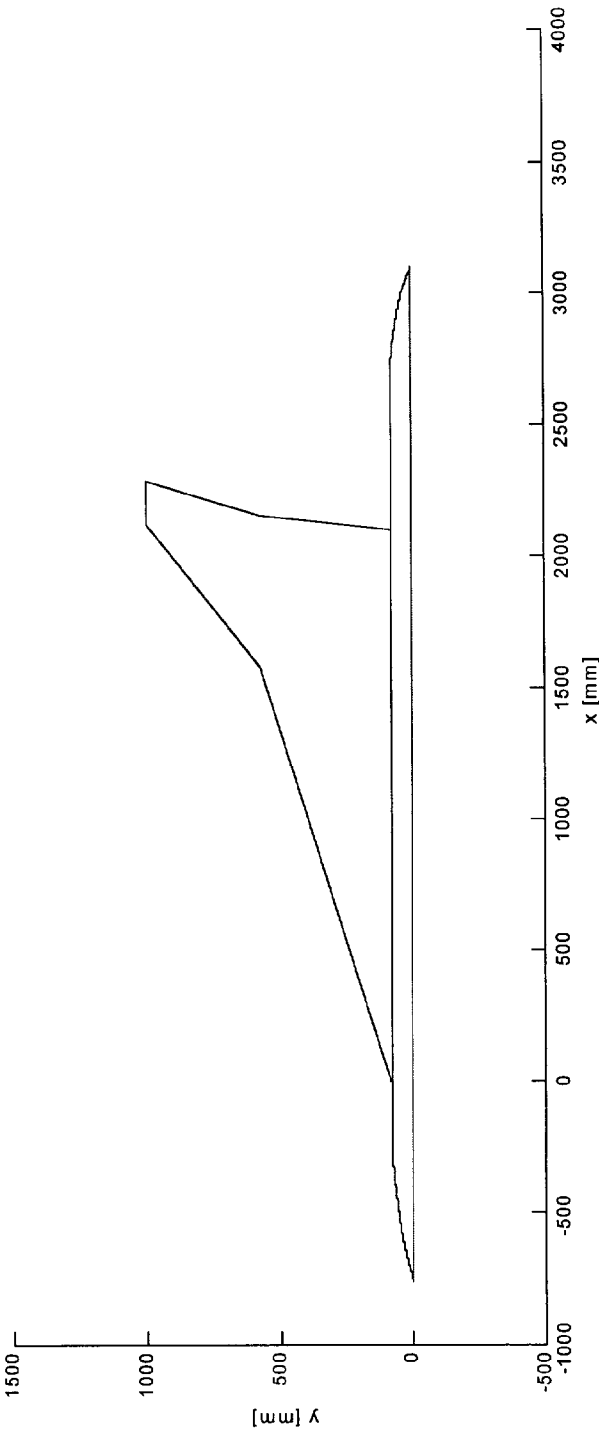


Figure 1 Semi-span Planform of SST Arrow Wing Model

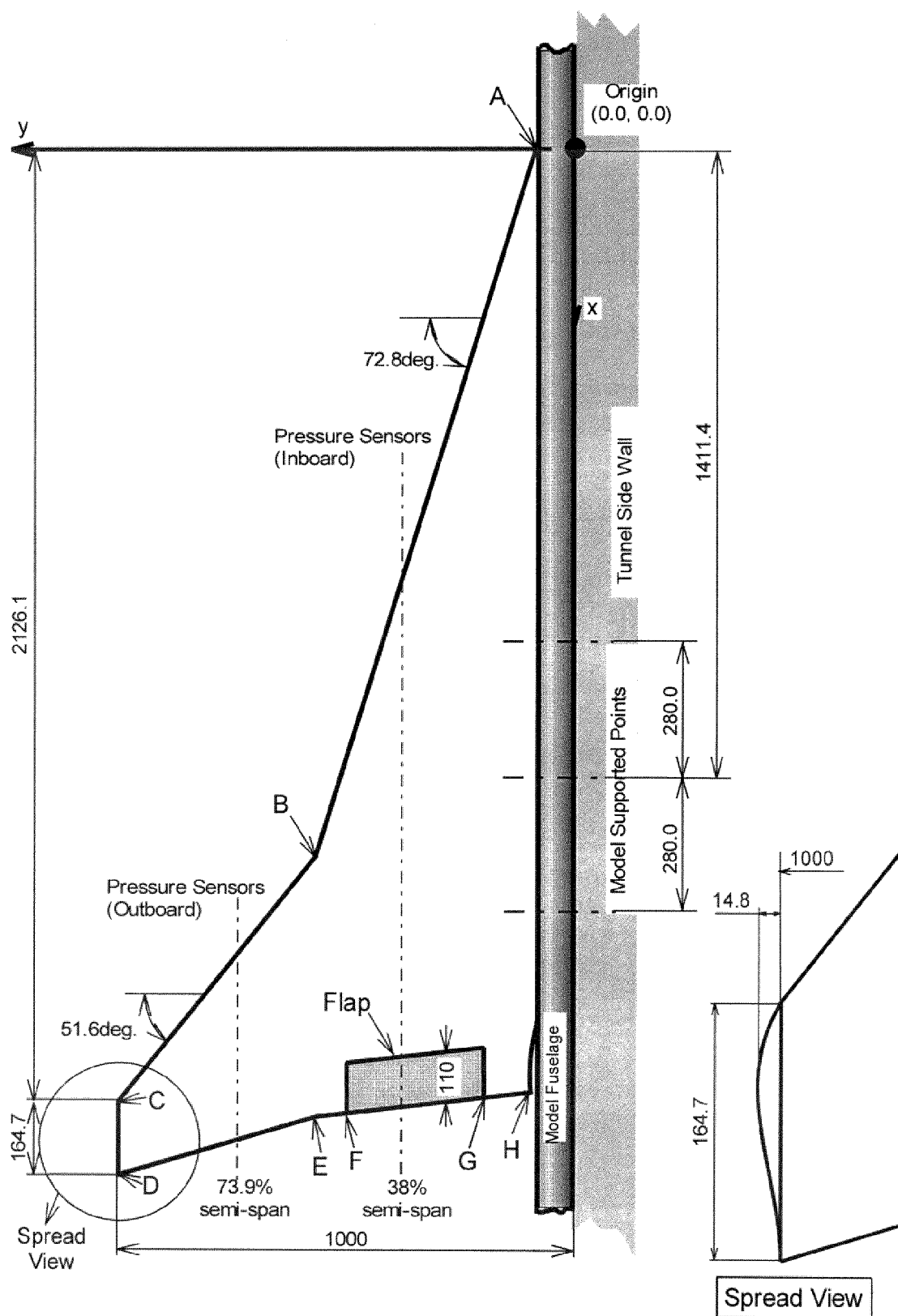
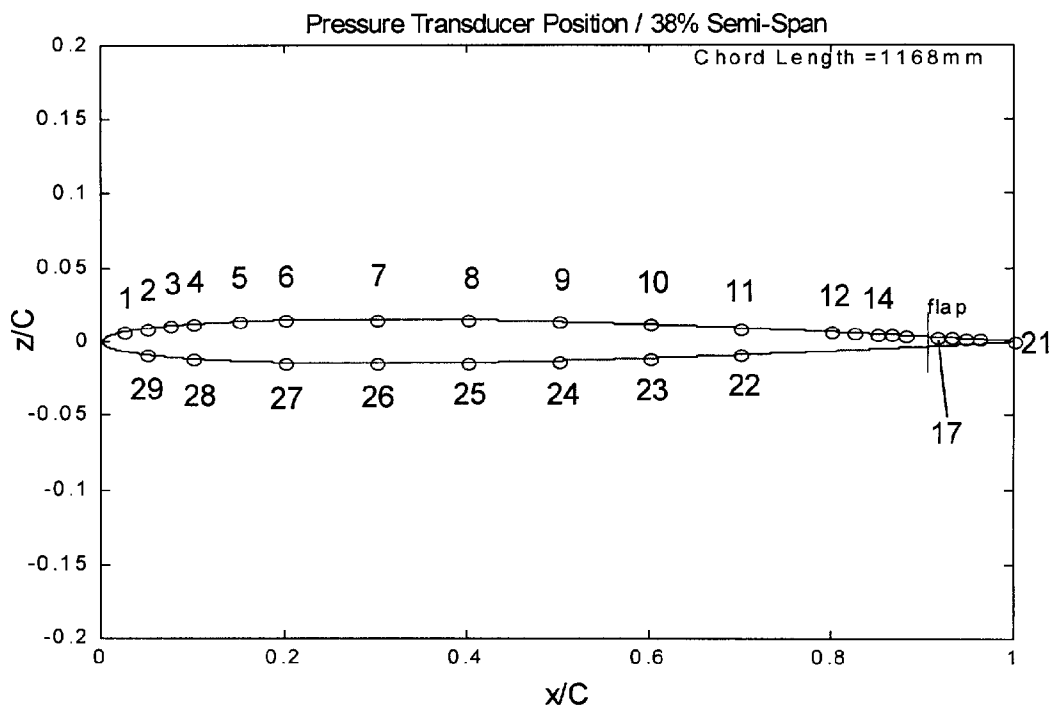
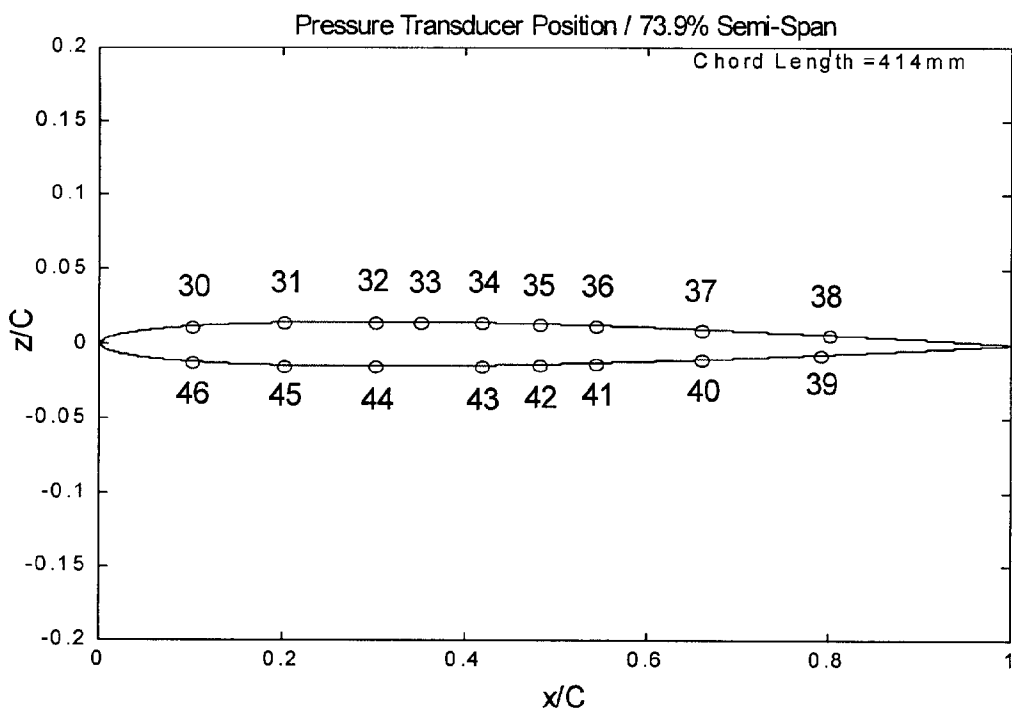


Figure 2 Model Planform ( wing part )



(a) 38 % semi-span



(b) 73.9 % semi-span

Figure 3 Pressure Orifice Positions

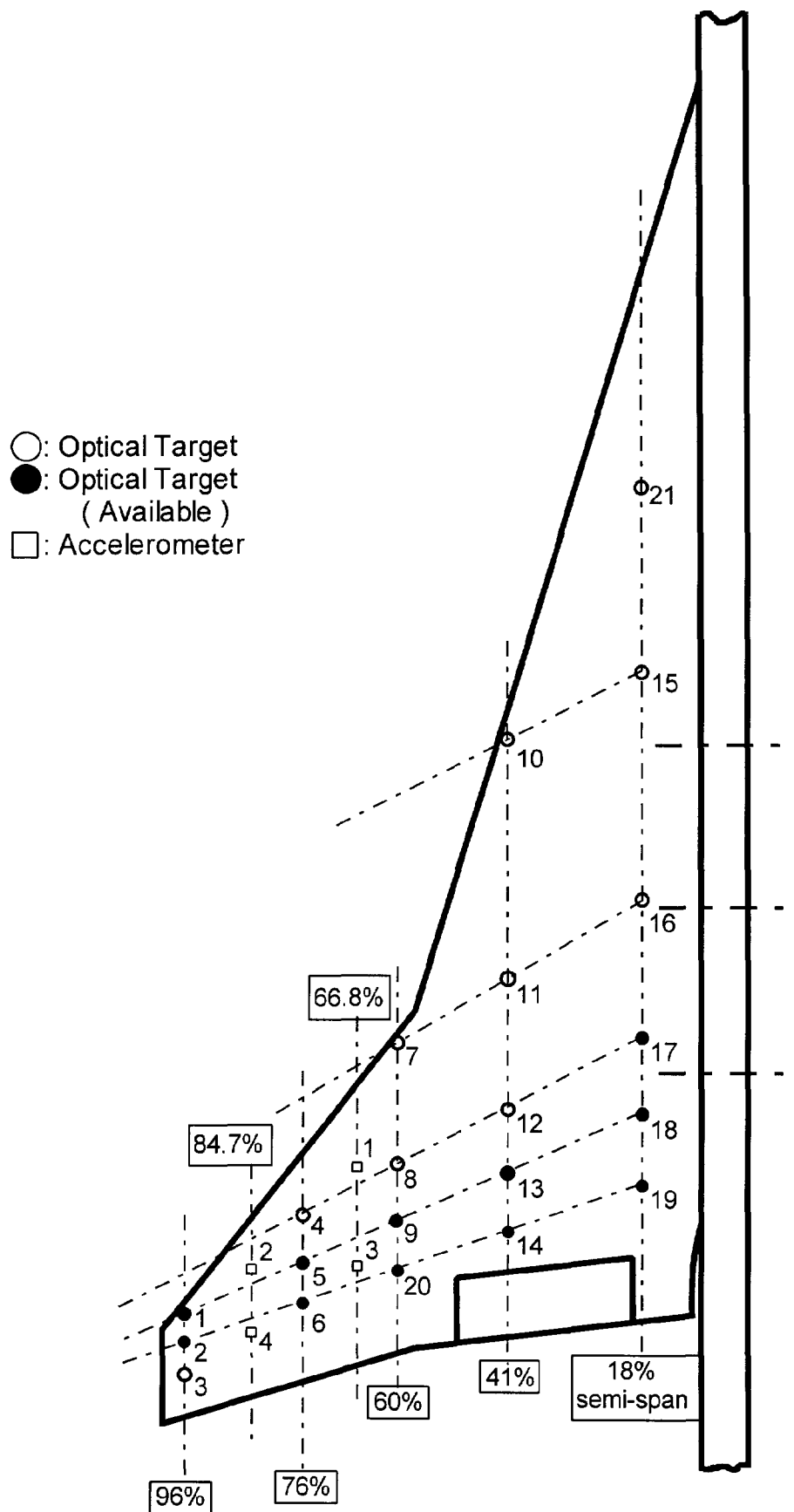


Figure 4 Positions of Optical Targets

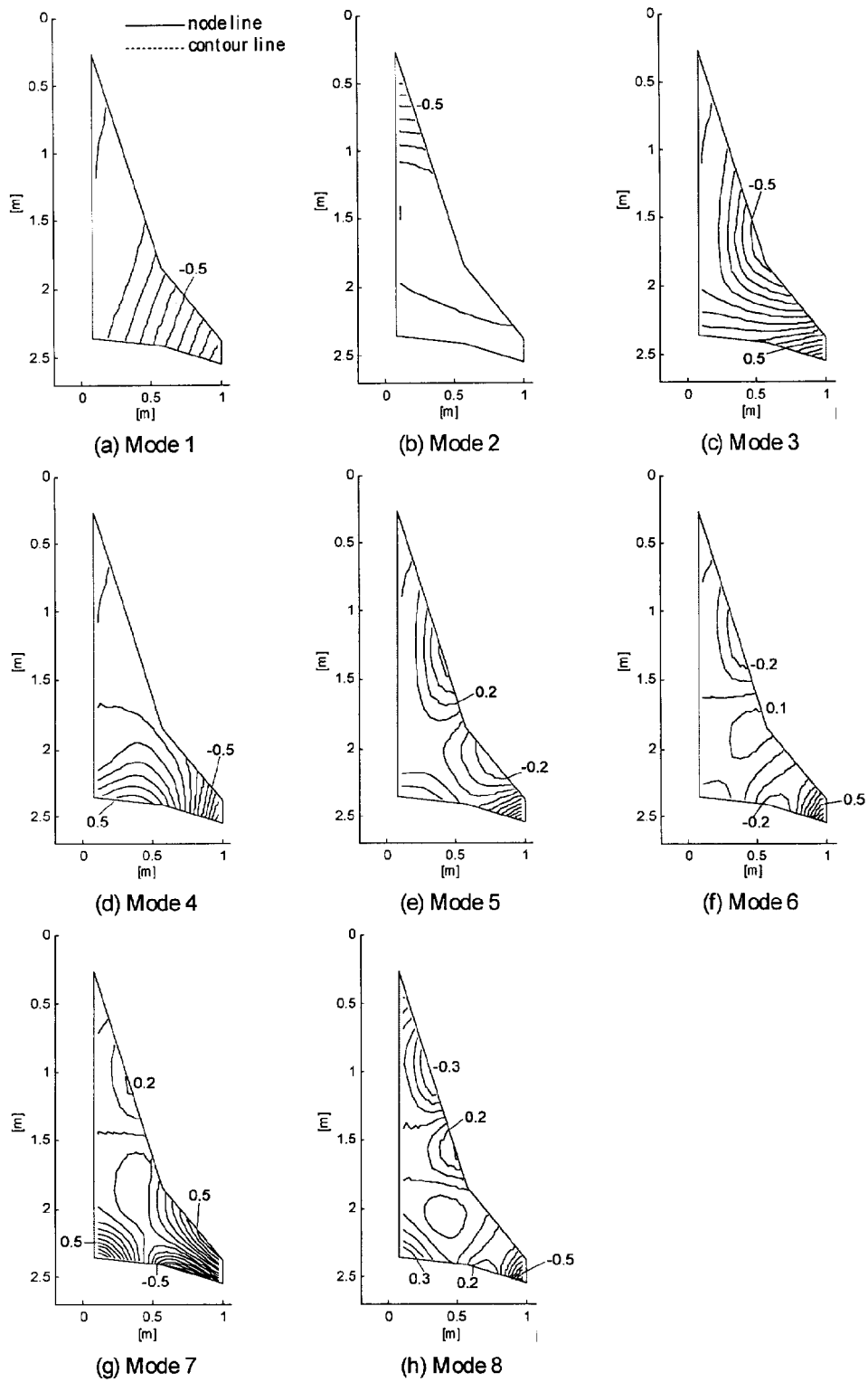
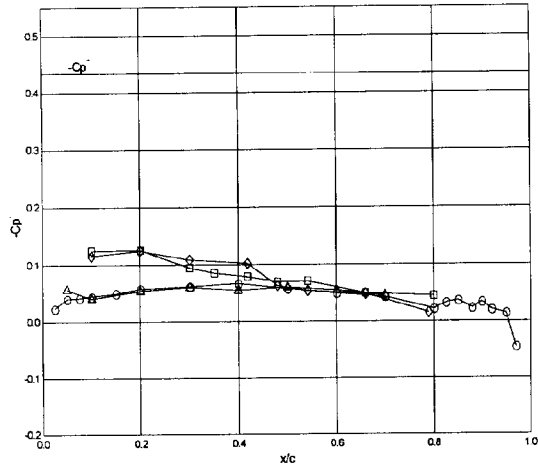
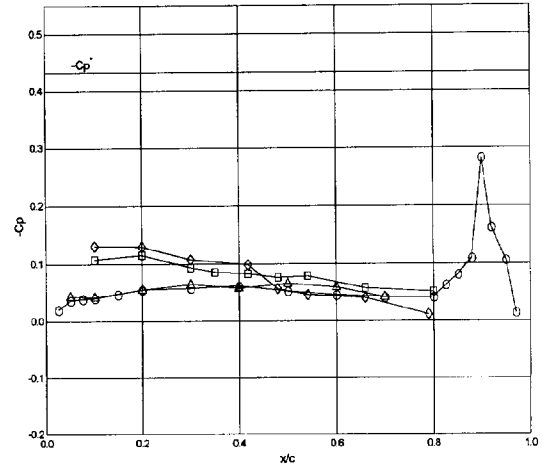


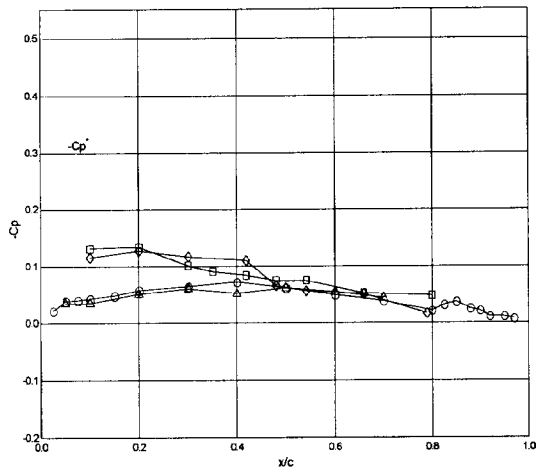
Figure 5 Model Natural Mode Contours Acquired by FEM  
( Contours are normalized with the maximum displacement )



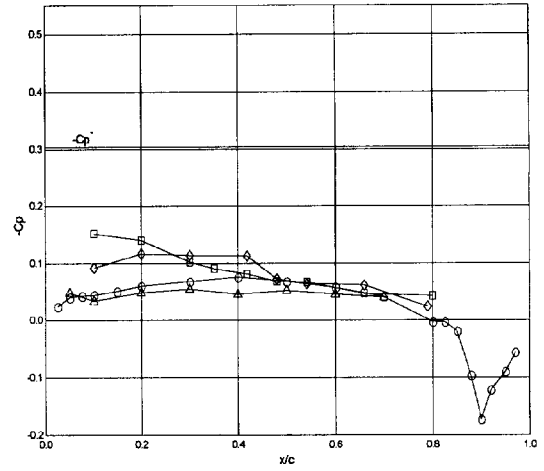
(a) AC100803



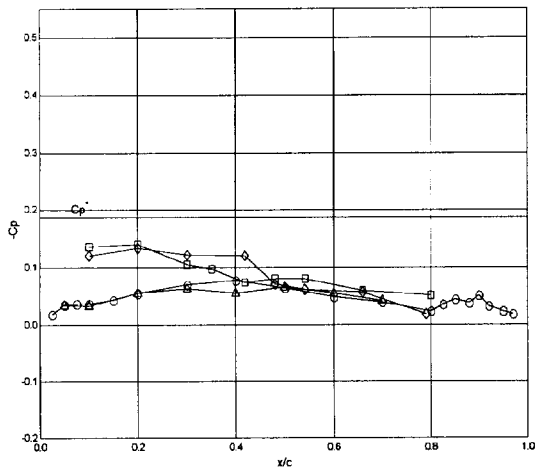
(b) AC100804



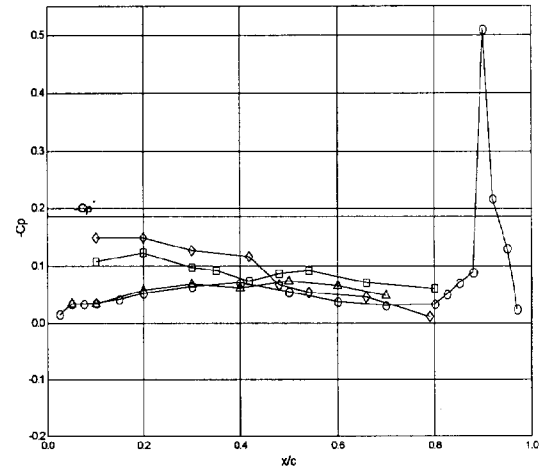
(c) AC100901



(d) AC100902



(e) AC100907



(f) AC100908

Figure 6 Steady Pressure Coefficient Distributions.  
( O: Inboard Upper , Δ: Lower , □: Outboard Upper, ◇: Lower )

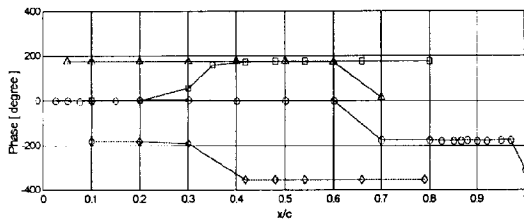
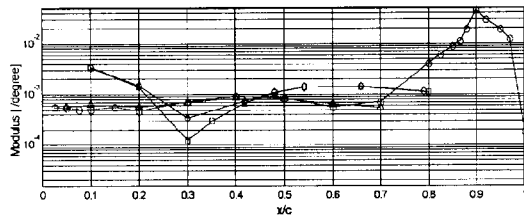
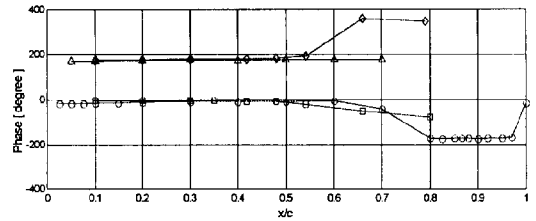
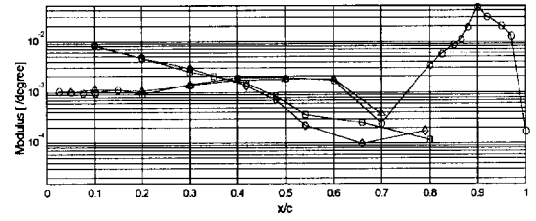
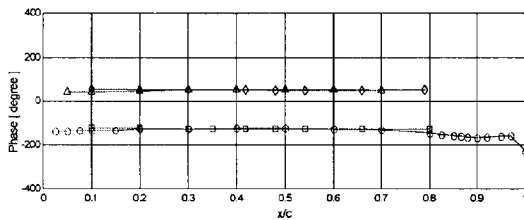
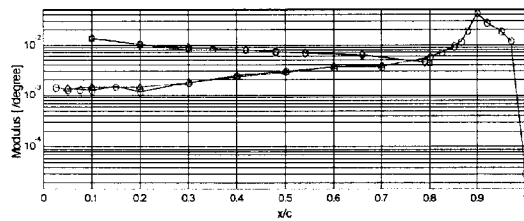
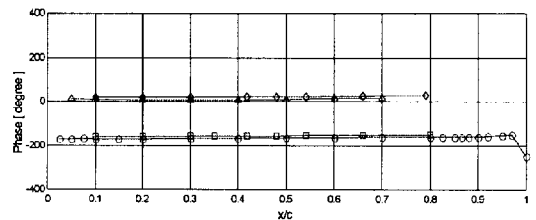
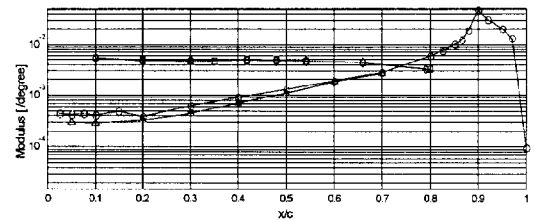
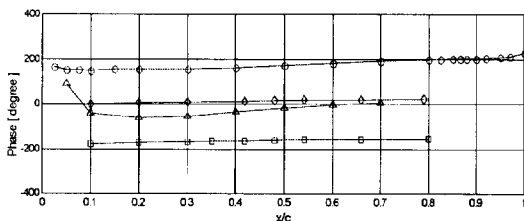
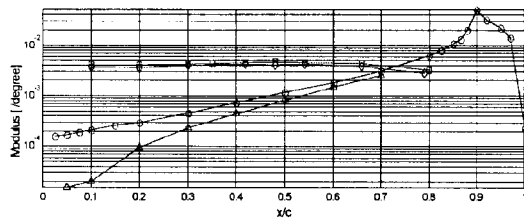
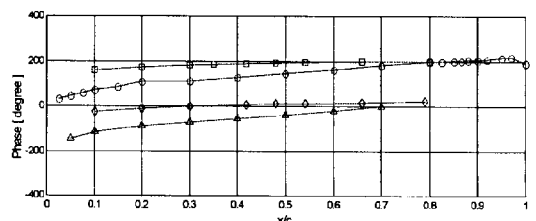
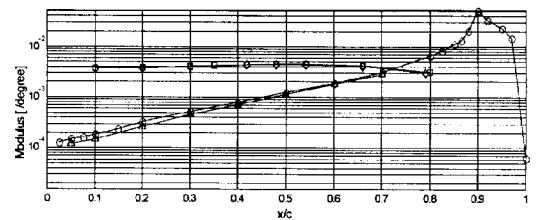
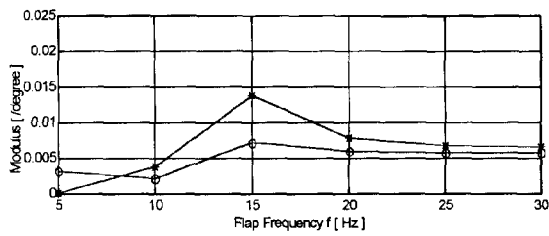
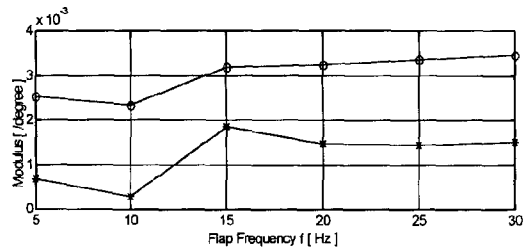
(a)  $f = 5$  [Hz](b)  $f = 10$  [Hz](c)  $f = 15$  [Hz](d)  $f = 20$  [Hz](e)  $f = 25$  [Hz](f)  $f = 30$  [Hz]

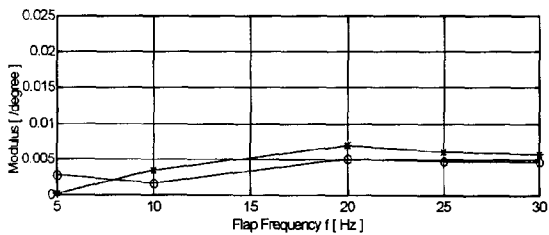
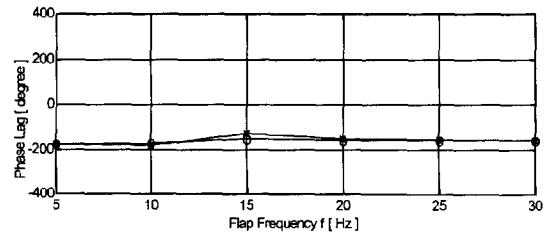
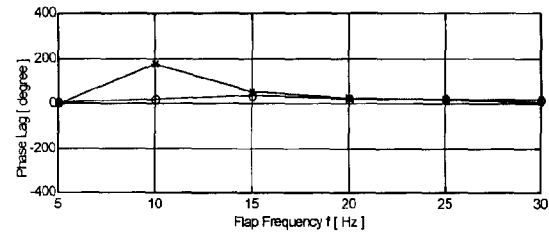
Figure 7.1 Unsteady Pressure Distributions.  $x/c$  vs Modulus & Phase.  
 Test Case AC100803  $M = 0.8002$ ,  $P_o = 79.925$  kPa,  
 $Re = 2.142 \cdot 10^7$ ,  $\alpha = 0$  deg.,  $\Delta = 0$  deg.  
 ( O: Inboard Upper ,  $\Delta$ : Lower ,  $\square$ : Outboard Upper ,  $\diamond$ : Lower )



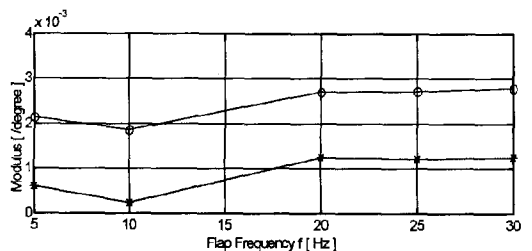
(a) AC100803, M=0.8002, CI



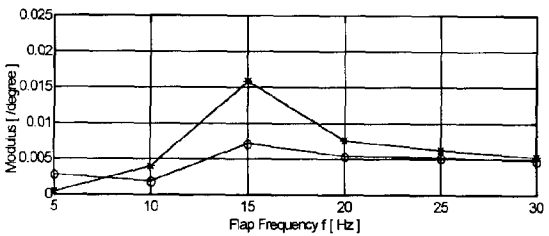
(b) AC100803, M=0.8002, Cm



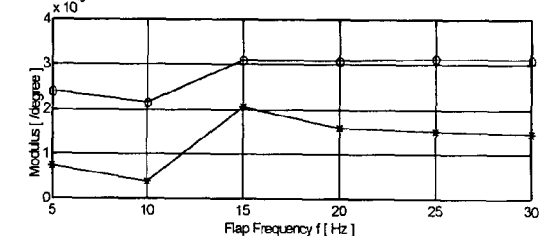
(c) AC100804, M=0.8004, CI



(d) AC100804, M=0.8004, Cm



(e) AC100901, M=0.8507, CI



(f) AC100901, M=0.8507, Cm

Figure 8.1 Unsteady Aerodynamic Force Coefficients.  
 $x/c$  vs Modulus & Phase.  
 ( O: Inboard, \*: Outboard )



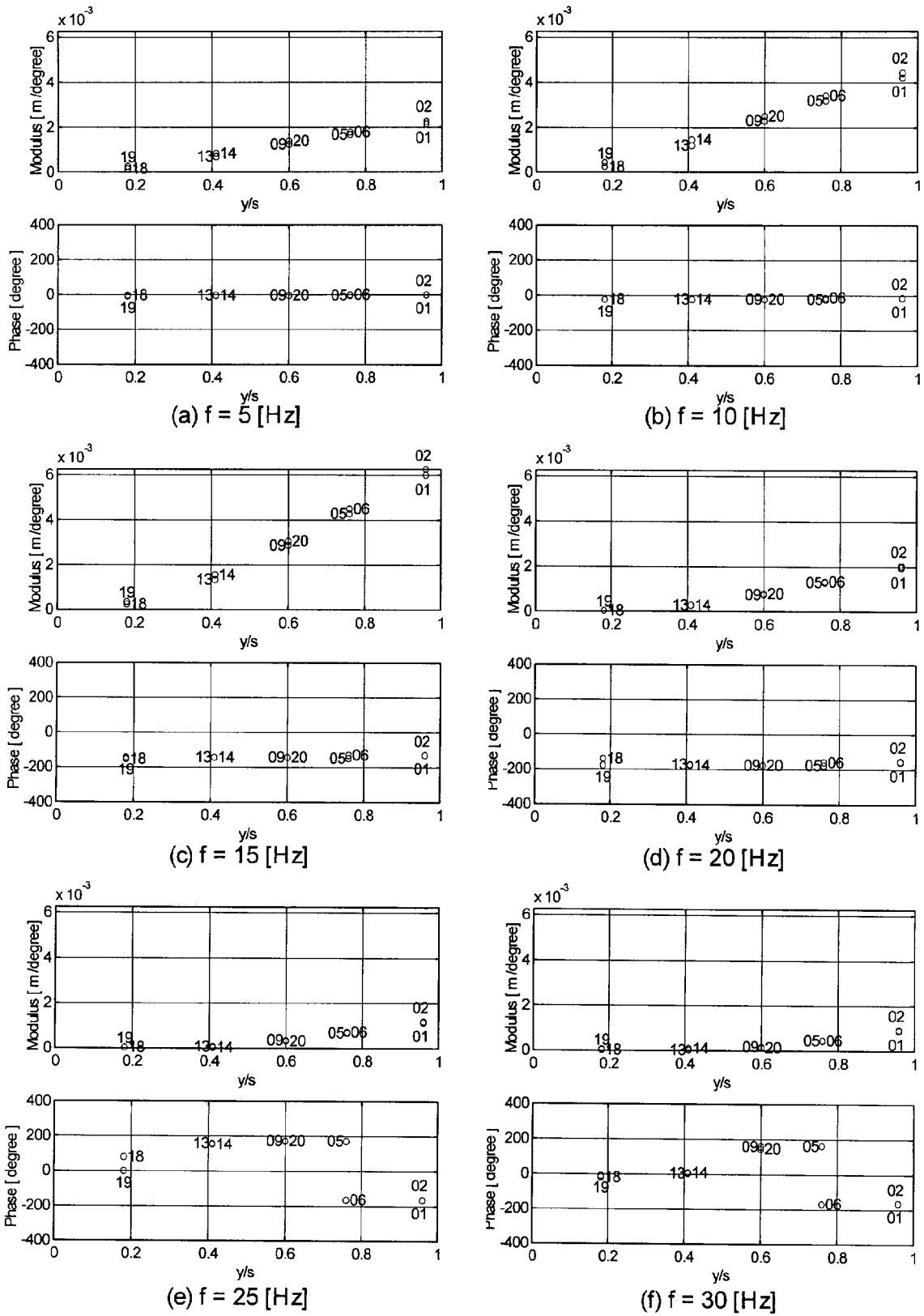


Figure 9.1 Unsteady Model Deformations.  $x/c$  vs Modulus & Phase.  
 Test Case AC100803  $M = 0.8002$ ,  $P_o = 79.925$  kPa,  
 $Re = 2.142 \times 10^7$ ,  $\alpha = 0$  deg.,  $\Delta = 0$  deg.